Torque-Speed Characteristic Estimation based on Gaussian Processes and Adaptive Sampling Strategy for Permanent Magnet Synchronous Machines

Marcelo D. Silva

Department of Electrical Engineering

Uppsala University

Uppsala, Sweden

marcelo.silva@angstrom.uu.se

Pedram Asef
e-Motion Laboratory
University College London
London, United Kingdom
pedram.asef@ucl.ac.uk

Oluwaseun A. Badewa

SPARK Laboratory

Pigman College of Engineering

University of Kentucky

Lexington, KY, USA

o.badewa@uky.edu

Rosemary E. Alden
SPARK Laboratory
Pigman College of Engineering
University of Kentucky
Lexington, KY, USA
rosemary.alden@uky.edu

Dan M. Ionel

SPARK Laboratory

Pigman College of Engineering

University of Kentucky

Lexington, KY, USA

dan.ionel@ieee.org

Abstract—Internal Permanent Magnet Synchronous Machines (IPMs) are widely used and typically optimized to meet specific performance requirements. Parameters such as base speed, maximum torque, and maximum speed commonly define the torquespeed characteristic of a given design. This study introduces a novel machine learning approach for statistically estimating the torque-speed characteristics of IPMs using Gaussian Process Regression (GPR), which models predictions as random variables. By leveraging uncertainty quantification, the study explores sampling strategies that enable the construction of a high-precision meta-model with minimal error and uncertainty. The proposed adaptive sampling strategy, combined with GPR, accurately estimates torque-speed characteristics and associated losses across the design space for the first time. This new method uses only a limited number of Finite Element Method (FEM)based simulations, showing high accuracy with 12 FEM-based simulations. The results demonstrate good agreement with full FEM evaluations and experimental measurements, validating the effectiveness of the proposed method.

Index Terms—Gaussian Process Regression, Torque-Speed Characteristics, Internal Permanent Magnet Synchronous Machine, Experimental Verification, FEM.

I. INTRODUCTION

The design of Internal Permanent Magnet Synchronous Machines (IPMs) typically involves meeting multiple performance metrics across a range of operating points. The design space often spans several dimensions, including both continuous variables and discrete decisions, such as the number of poles, the number of slots per pole, and the phase number. This combination of high-dimensional inputs, multiple outputs, and

Funded by the StandUp for Energy strategic government initiative, the Swedish Electromobility Center, and by the US National Science Foundation (NSF) Graduate Research Fellowship under Grant No. 2239063.

diverse objectives necessitates a large number of evaluations, not only across different designs, but also multiple evaluations of the same design. As a result, relying solely on Finite Element Method (FEM)-based simulations becomes both time-consuming and computationally impractical [1].

To address this challenge, meta-models can be developed to enable evaluation of IPM performance with significantly reduced computational effort. These meta-models may be based on regression techniques [2], physical governing equations [3], or artificial neural networks [4]. Alternatively, Gaussian Process Regression (GPR) has emerged as a powerful approach for meta-modeling due to its efficient use of the data [1]. It has been applied in various contexts, ranging from general meta-modeling tasks [5] to fill-factor maximization [6].

However, the data used to build the aforementioned metamodels impacts their performance and data efficiency. The selection of these data points can either be predetermined (referred to as static) or be based on the meta-model's performance during the training process (referred to as adaptive). In this regard, GPR offers the ability to quantify prediction uncertainty [7], which is often used to guide adaptive sampling strategies to improve model performance. This study proposes a novel adaptive sampling strategy based on uncertainty quantification. The developed meta-model, built using the proposed sampling strategy, aims to accurately compute performance metrics at selected operating points while minimizing the number of FEM-based evaluations required. In typical GPRbased approaches, uncertainty is computed directly on the meta-model outputs. However, the proposed method treats GPR predictions as random variables and applies uncertainty propagation rules to estimate uncertainty in key performance

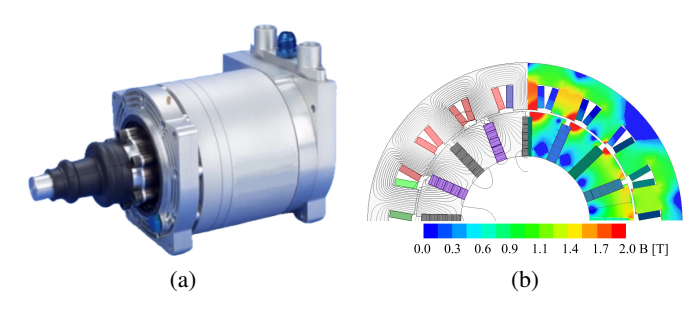


Fig. 1: IPM motor with ultra-high specific torque serves as the benchmark for this analysis. Shown in (a) is the prototype developed during the initial phase of Formula E. (b) illustrates the magnetic field distribution within the motor's cross-section, highlighting flux lines and regions where flux density exceeds 2 T, indicating significant magnetic saturation.

metrics, specifically, torque and loss components. Thus, focusing on reducing uncertainty at the most relevant operating points selected by the optimization problem and goals.

The torque-speed characteristics obtained using the proposed adaptive sampling strategy are compared against those derived from standard techniques, including Posterior Standard Deviation, quasi-random sampling heuristics, and full FEM-based evaluations. The torque-speed curves are computed using Maximum Torque per Ampere (MTPA) [8] and field weakening [9] operating points, along with predictions of associated loss components. Furthermore, the results are validated against experimental measurements.

Section II introduces the spoke-type IPM used as the benchmark in this study. Section III then outlines the implementation of Gaussian Process Regression (GPR) and its foundational concepts. Section IV presents the proposed adaptive sampling strategy in detail, highlighting its differences from standard approaches. Finally, Section V discusses the results, comparing the proposed strategy with alternative sampling techniques and experimentally validating its performance.

II. BENCHMARK IPM MOTOR

This study uses an IPM prototype motor as a reference model. Originally developed for the first generation of Formula E vehicles, the motor was later refined, with further details available in [10] and [11]. The motor features a spoke-type rotor with 16 poles and a three-phase winding composed of concentrated coils distributed across 18 stator teeth, as illustrated in Fig. 1. It is capable of delivering up to 110 Nm of torque, reaching speeds of 12,000 rpm, and handling 325 Arms, powered by a 650 V DC bus [11]. For this analysis, a base speed of 3,500 rpm was selected. Notably, the motor design achieves a record-high specific torque and exhibits significant magnetic saturation, making it a suitable candidate for investigating nonlinear magnetic behavior.

Based on this prototype, eight geometric parameters were selected for inclusion in the design space. The specific value ranges for these parameters are presented in Table I, where k_{si} is the quotient between the stator inner and outer diameter;

TABLE I: Details on Geometric Variables

Variables	Maximum	Minimum	Prototype
k_{si} [-]	0.75	0.6	0.704
h_g [mm]	2.5	0.7	1
k_{w_t} [-]	0.75	0.45	0.662
$k_{h_{pm}}$ [-]	0.95	0.55	0.775
$k_{w_{pm}}$ [-]	0.6	0.2	0.388
$k_{w_{br}}$ [-]	0.65	0.35	0.5
d_{br} [mm]	3	1.5	2.5
h_y [mm]	15	7	10.7

 h_g , the air gap length; k_{w_t} , the quotient between the stator teeth width and its maximum; $k_{h_{pm}}$, the quotient between the PMs' height and the maximum for PMs' height; $k_{w_{pm}}$, the quotient between the PMs width with the rotor pole; $k_{w_{br}}$, the proportion of the rotor slot opening in relation to the PMs' width; d_{br} , the distance between the rotor's surface and the PMs' top; and h_y , the distance between the top of the stator slot and the outer stator diameter.

III. GAUSSIAN PROCESS REGRESSION AND ADAPTIVE SAMPLING STRATEGIES

A Gaussian Process (\mathcal{GP}) is a probabilistic model defined by a collection of random variables, each of which follows a multivariate normal distribution. This framework is particularly effective for regression tasks, as it enables the \mathcal{GP} to be trained using observed data to make predictions [7]. Mathematically, a \mathcal{GP} can be represented as:

$$f(\mathbf{x}) \sim \mathcal{GP}(m(\mathbf{x}), k(\mathbf{x}, \mathbf{x}')),$$
 (1)

where m(x) is the mean function; and k(x, x'), the covariance function. The mean function m(x) is defined as linear:

$$m(\mathbf{x}) = W\mathbf{x} + B,\tag{2}$$

where W and B are constants learned during training.

Following the definition of \mathcal{GP} , an evaluation based on it and an input $\mathbf{x}' = [i_d, i_q, \omega_e]$, where $i_d = -I_{ph} sin(\gamma)$, $i_q = I_{ph} cos(\gamma)$, I_{ph} is the phase current and ω_e is the electrical speed, can be described by a Gaussian distribution. Resulting in:

$$\psi_d(\mathbf{x}') \sim \mathcal{N}(\mu_d, \sigma_d^2),$$
 (3)

$$\psi_q(\mathbf{x}') \sim \mathcal{N}(\mu_q, \sigma_q^2),$$
 (4)

for the flux linkage maps prediction. Similarly, for losses:

$$L_{copper}(\mathbf{x}') \sim \mathcal{N}(\mu_{cp}, \sigma_{cp}^2),$$
 (5)

$$L_{core}(\mathbf{x}') \sim \mathcal{N}(\mu_{co}, \sigma_{co}^2),$$
 (6)

$$L_{solid}(\mathbf{x}') \sim \mathcal{N}(\mu_s, \sigma_s^2),$$
 (7)

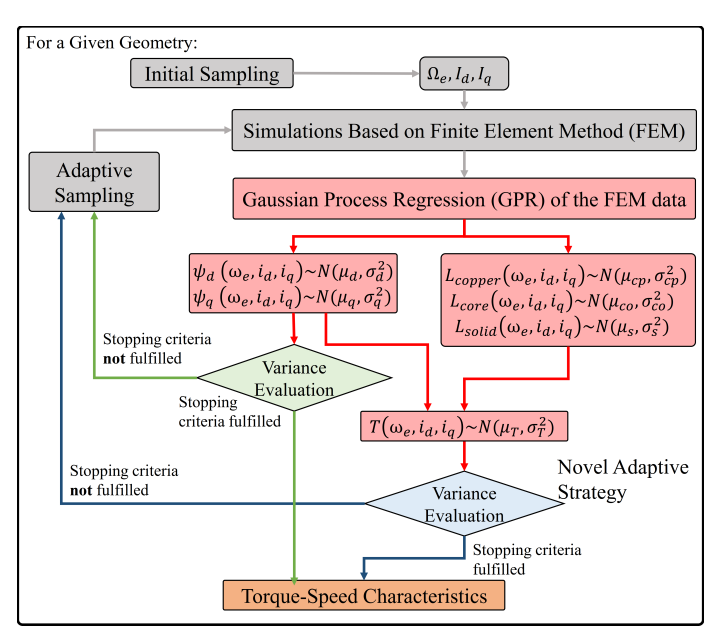


Fig. 2: Illustration of the meta-model structure with the blue elements indicating the novel adaptive sampling strategy. The green indicates the traditional approach to adaptive sampling when using GPR. The FEA simulations and other auxiliary steps are identified in gray. The pink is representative of GPR predictions and the computations using them. The torque-speed characteristic is the output of this meta-model.

where L_{copper} are stator winding copper losses component; L_{core} , core losses component; and L_{solid} , the eddy losses in the permanent magnets (PMs) component.

Adaptive sampling strategies leverage the \mathcal{GP} 's predictive uncertainty to guide the sampling process. When used in optimization contexts, such strategies ideally balance exploration and exploitation of the output domain. However, in this study, the \mathcal{GP} is employed to explore the output domain without selecting specific inputs, so the focus is solely on exploration-oriented sampling strategies. Within this category, both Upper Confidence Bound (UCB) [12] and Posterior Standard Deviation (PSD) [7] are well-known approaches.

These two strategies differ in the information used to guide sampling. UCB depends on the predicted mean and the associated uncertainty, allowing it to shift toward exploitation when uncertainty is low. In contrast, PSD relies exclusively on uncertainty, making it purely exploratory. For this study, the objective is to reduce uncertainty across the entire output domain, described in equations (3)–(7), thus being an exploratory problem. Therefore, the novel adaptive sampling strategy introduced in Section IV is based on PSD.

In addition to the sampling strategy employed, the \mathcal{GP} 's mean functions were optimized independently for each input dimension. The covariance function $k(\mathbf{x}, \mathbf{x}')$ that yielded the best results was the *Matérn 5/2 kernel*. Since the training data was generated using FEM-based simulations [13], it is considered noise-free, and no inter-task transfer effects are present [14]. The initial dataset was constructed using a quasi-random

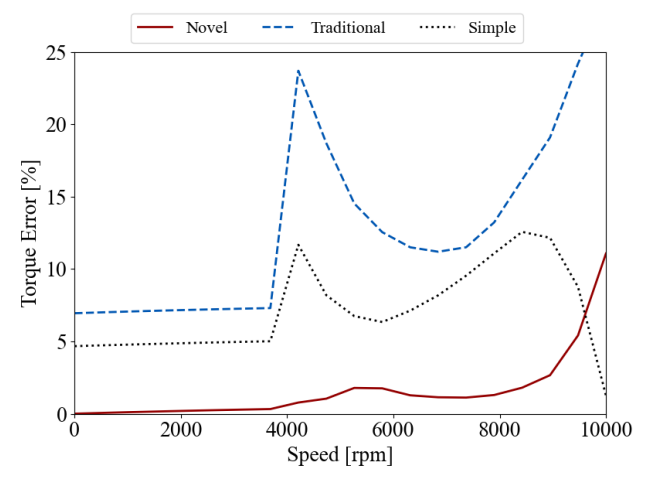


Fig. 3: For the alternative geometry: Torque error comparison between the predictions by the \mathcal{GP} trained using the proposed adaptive sampling strategy, by the \mathcal{GP} trained using standard PSD and by the \mathcal{GP} trained using simple sampling.

sampling heuristic — Latin Hypercube Sampling (LHS) — combined with boundary sampling to ensure coverage of the design space. This initialization, illustrated in Fig. 2, provides a robust foundation for subsequent adaptive refinement.

IV. NOVEL ADAPTIVE SAMPLING STRATEGY

The comparison between the standard PSD approach and the novel adaptive sampling strategy proposed in this study is illustrated in Fig. 2. In the standard PSD, the sampling process is guided by the uncertainty of the \mathcal{GP} outputs, which in this study are the flux linkage and loss components. Given sufficient computational resources, this approach can generate comprehensive maps with low uncertainty and high accuracy. However, control algorithms for electric machines, such as Maximum Torque per Ampere (MTPA) and field weakening, are designed to operate IPMs efficiently at specific working points. As a result, not all combinations of ω_e , i_d , and i_q are equally relevant or likely to be used in practice.

The idea of restricting the flux linkage domain to regions of interest has previously been proposed as a basis for building meta-models using regression techniques [2]. However, that study did not address how MTPA and field weakening trajectories are computed, and the method was applied to a single machine design. In contrast, this work explicitly incorporates the calculation of MTPA and field weakening trajectories, discussed in this section and evaluated across multiple IPM designs in Section V. This broader scope enhances the generalization and practical relevance of the proposed method.

The proposed adaptive sampling strategy, like PSD, uses uncertainty to guide the sampling process. However, instead of focusing on the uncertainty of the direct \mathcal{GP} outputs, it propagates this uncertainty through the governing physical equations to estimate uncertainty in the key performance metric: the torque-speed characteristic. This allows the sampling to be more targeted and aligned with the actual design objectives. The torque expression based on flux linkages is given by:

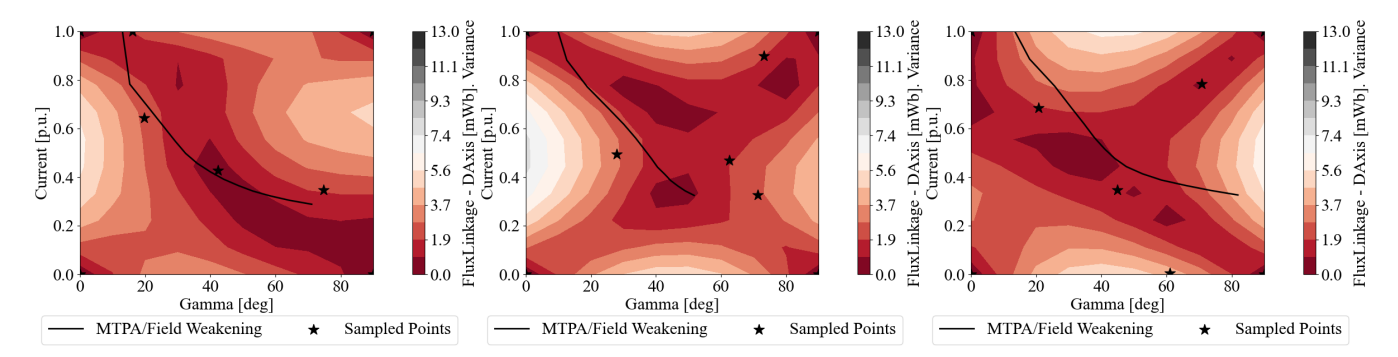


Fig. 4: For the prototype geometry: Left (a): Variance of ψ_d from the \mathcal{GP} trained using the proposed adaptive sampling strategy. Middle (b): Variance of ψ_d from the \mathcal{GP} trained using standard PSD. Right (c): Variance of ψ_d from the \mathcal{GP} trained using simple sampling.

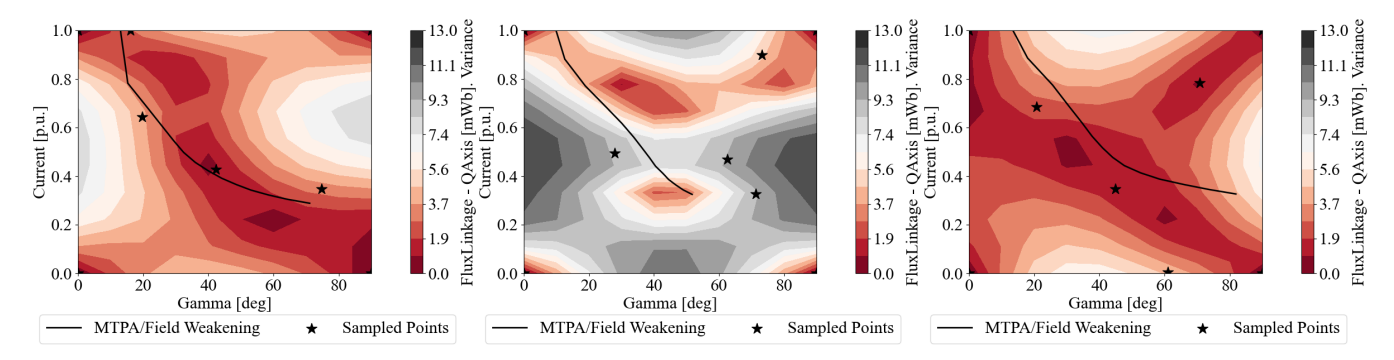


Fig. 5: For the prototype geometry: Left (a): Variance of ψ_q from the \mathcal{GP} trained using the proposed adaptive sampling strategy. Middle (b): Variance of ψ_q from the \mathcal{GP} trained using standard PSD. Right (c): Variance of ψ_q from the \mathcal{GP} trained using simple sampling.

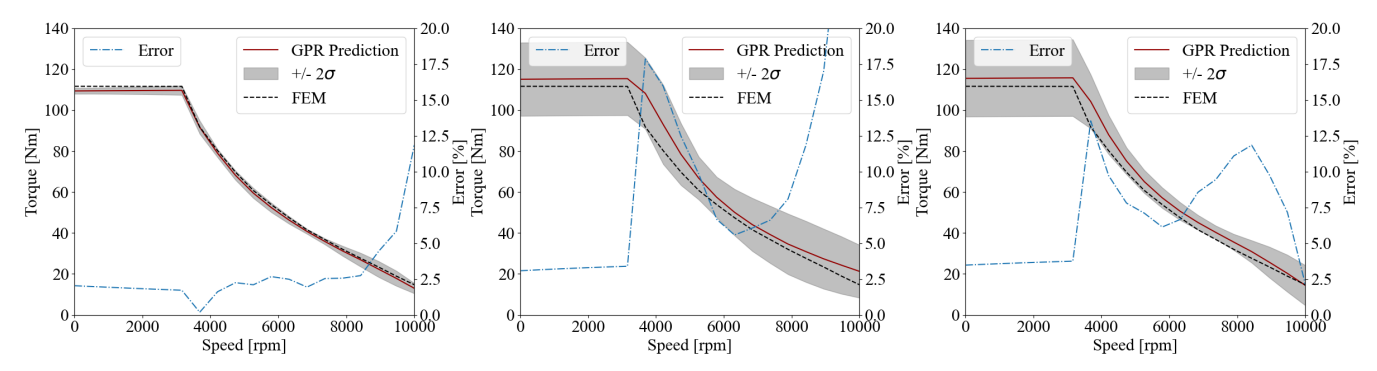


Fig. 6: For the prototype geometry: Left (a): Torque prediction (solid line) by the \mathcal{GP} trained using the proposed adaptive sampling strategy. Middle (b): Torque prediction (solid line) by the \mathcal{GP} trained using standard PSD. Right (c): Torque prediction (solid line) by the \mathcal{GP} trained using simple sampling.

$$T_e = 1.5p[\psi_d i_q - \psi_q i_d],\tag{8}$$

and, in combination with equations (3) and (4), torque can be defined as a random variable:

$$T_e \sim \mathcal{N}(\mu_t, \sigma_t^2) \\ \sim \mathcal{N}(1.5p(\mu_d i_q - \mu_q i_d), (1.5p)^2(\sigma_d^2 i_q^2 + \sigma_q^2 i_d^2)),$$
 (9)

where p is the number of pole pairs. As a result, the proposed adaptive sampling strategy focuses specifically on minimizing

 σ_t^2 , rather than the individual uncertainties σ_d^2 , σ_q^2 , σ_{cp}^2 , σ_{co}^2 , or σ_s^2 as in the standard PSD approach.

This focus on the uncertainty of a key performance metric, rather than intermediate variables, enables more targeted and efficient sampling. Additionally, it allows for a reduction in the input domain $\mathbf{x}' = [i_d, i_q, \omega_e]$, concentrating efforts on the most relevant regions for a given application. By focusing on selected areas of the input space, the meta-model can achieve higher accuracy without requiring a larger dataset.

In this study, the regions of interest are defined by the MTPA

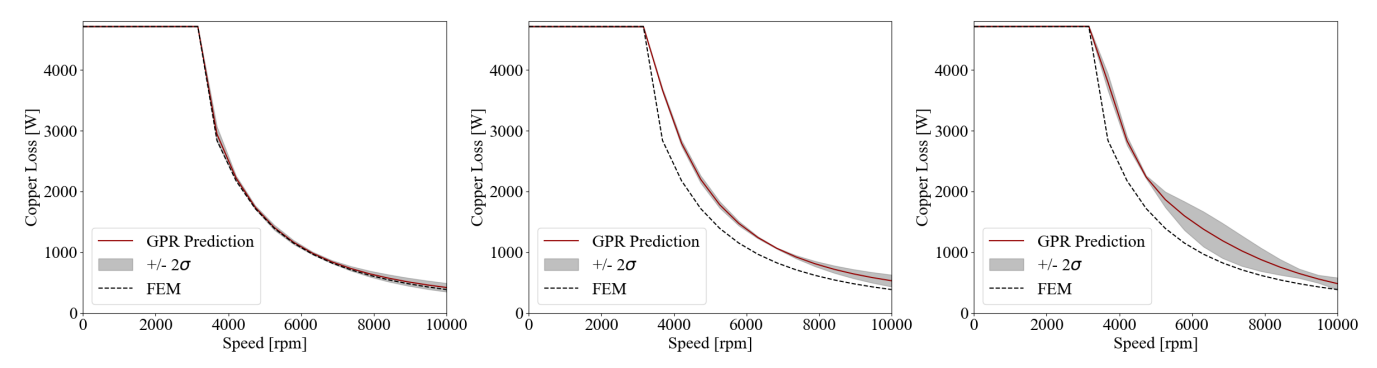


Fig. 7: For the prototype geometry: Left (a): Copper losses prediction (solid line) by the \mathcal{GP} trained using the proposed adaptive sampling strategy. Middle (b): Copper losses prediction (solid line) by the \mathcal{GP} trained using standard PSD. Right (c): Copper losses prediction (solid line) by the \mathcal{GP} trained using simple sampling.

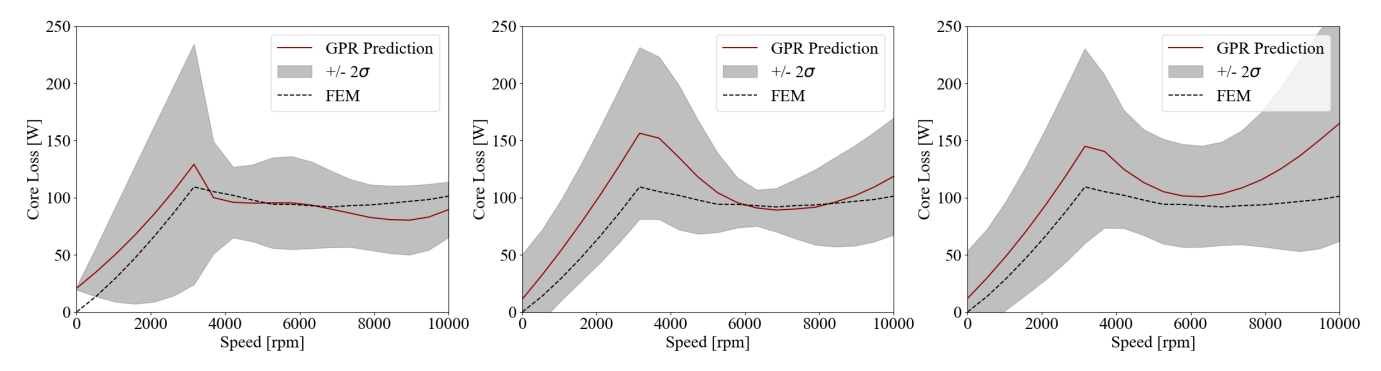


Fig. 8: For the prototype geometry: Left (a): Core losses prediction (solid line) by the \mathcal{GP} trained using the proposed adaptive sampling strategy. Middle (b): Core losses prediction (solid line) by the \mathcal{GP} trained using standard PSD. Right (c): Core losses prediction (solid line) by the \mathcal{GP} trained using simple sampling.

and field weakening operating points. The meta-model uses the initial sampling data to estimate which combinations of ω_e , i_d , and i_q correspond to these points. It then computes the torque uncertainty for each of these combinations using equation (9). The adaptive sampling strategy selects the input combination within the region of interest that yields the highest torque uncertainty, evaluates it using FEM, and incorporates the result into the dataset to retrain the GPR.

V. RESULTS AND DISCUSSION

The performance of the \mathcal{GP} trained with the proposed adaptive sampling strategy is evaluated based on its ability to compute torque-speed characteristics and predict losses at those points. Its performance is compared to a \mathcal{GP} trained with standard PSD and another trained with only initial sampling, as described in Section III. Each \mathcal{GP} was trained with twelve FEM-based simulations.

To start, it was demonstrated that the proposed approach to adaptive sampling yielded good results for several machine designs in the domain, the torque estimation error presented in Fig. 3 is the result of a similar analysis done for the random machine design with the following geometric dimensions: $k_{si} = 0.650$, $h_g = 0.800$, $k_{wt} = 0.564$, $k_{h_{pm}} = 0.875$, $k_{w_{pm}} = 0.388$, $k_{w_{br}} = 0.400$, $d_{br} = 2.00$ and $h_y = 12.4$. The high accuracy of the torque estimation with the proposed adaptive

sampling strategy is achieved because it does not rely on any prior knowledge of the IPM being analyzed.

The goal of the proposed adaptive sampling strategy is to guide the sampling process toward the area of interest. The MTPA and field weakening operating points (i.e., the area of interest) are computed based on each \mathcal{GP} 's estimation of ψ_d and ψ_q , and are illustrated in Fig. 4 and Fig. 5. These figures clearly show that the lines representing the area of interest pass through regions of lower variance, σ_d^2 and σ_q^2 , when the \mathcal{GP} is trained using the proposed adaptive sampling strategy. The sampling points selected by this strategy are also densely concentrated around the area of interest.

Re-examining the MTPA and field weakening points computed under each sampling scenario reveals significant differences in the identified working points. Consequently, the resultant torque-speed characteristics are also significantly distinct, as can be seen in Fig. 6. The \mathcal{GP} trained using the proposed adaptive sampling strategy presents an average error of 2.8%; trained using PSD presents an average error of 10.7%; and trained using simple sampling presents an average error of 6.8%. The uncertainty of the predictions of the \mathcal{GP} trained using the proposed adaptive sampling strategy is negligible, which is not the case for the other training scenarios. These results express the high performance of the proposed solution.

The prediction error of the torque-speed characteristics

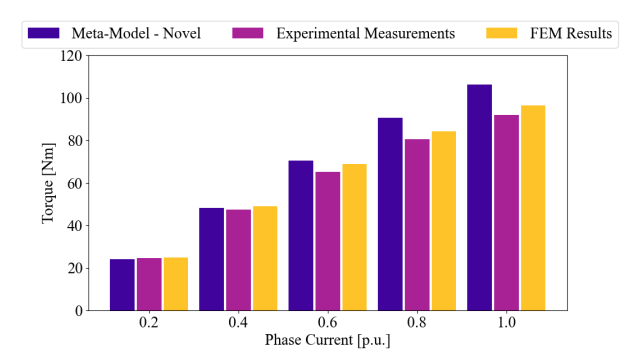


Fig. 9: Torque with $i_q = I_{ph}$ and $i_d = 0$ A for different I_{ph} .

presented in Fig. 6(a) and Fig. 3 demonstrates an extremely low error value for the maximum torque prediction (<0.5%), and an error less than 3% for more than 90% of the speed range. Additionally, the average error for the estimation of the torque-speed characteristic is reduced up to 80% using the proposed technique, requiring only three extra FEM-based simulations, when compared with a previous solution [2].

The loss components are estimated at the torque-speed characteristic working points, as defined in equations (5)–(7) and illustrated in Fig. 2. As previously demonstrated, the \mathcal{GP} trained using the proposed adaptive sampling strategy yielded lower errors in estimating the copper loss component (Fig. 7), core loss component (Fig. 8), and solid loss component (not shown due to space limitations). In addition to the reduced error, the associated uncertainty was also lower. Thus, the results suggest that the proposed sampling strategy can support not only performance optimization but also more informed design trade-offs involving energy efficiency.

The experimental measurements reported in [10] and [11] are compared with FEM simulations and the meta-model output generated using the proposed adaptive sampling strategy, as shown in Fig. 9. It is important to note that this comparison focuses on operating points where $i_d=0$ A, consistent with the conditions of the experimental measurements. Redefining the region of interest required reconstructing the dataset and retraining the \mathcal{GP} , further demonstrating the flexibility of the proposed approach in adapting to different working points of interest. Nevertheless, Fig. 9 demonstrates that the meta-model trained with the proposed strategy successfully predicts both the experimental and FEM results, with an average error of 4.6%. However, at higher current levels, the model appears to struggle with accurately capturing the effects of strong magnetic saturation, with an error of 15.2%.

VI. CONCLUSION

This study proposes a novel adaptive sampling strategy to be used in the construction of \mathcal{GP} -based meta-models, developed to achieve higher fidelity in the performance parameters for the working points of interest based on 12 FEM-based simulations. The proposed adaptive sampling strategy demonstrated improved performance in predicting torque-speed characteristics and loss components when compared with other well-established adaptive sampling strategies, such

as PSD. Additionally, the study showed that the method applies to a wide range of IPM designs and working points of interest, highlighting the flexibility and generality of the approach. Furthermore, the results showed good agreement with experimental measurements.

In comparison with previous data-efficient meta-modeling strategies, the method achieved a significant reduction in prediction error up to 80%, using only three additional FEM-based simulations. Therefore, the proposed solution showed a strong generalization capability across different IPM designs.

ACKNOWLEDGMENT

The support of the StandUp for Energy strategic government initiative, the Swedish Electromobility Center, and in the US of the National Science Foundation (NSF) Graduate Research Fellowship under Grant No. 2239063 is gratefully acknowledged. Any opinions, findings, and conclusions or recommendations expressed in this material are those of the authors and do not necessarily reflect the views of the sponsoring organizations.

REFERENCES

- M. Cheng, X. Zhao, M. Dhimish, W. Qiu, and S. Niu, "A review of data-driven surrogate models for design optimization of electric motors," *IEEE Transactions on Transportation Electrification*, pp. 1 – 1, 2024.
- [2] B. Praslicka, N. Taran, and C. Ma, "An ultra-fast method for analyzing IPM motors at multiple operating points using surrogate models," *IEEE Transportation Electrification Conference and Expo (ITEC)*, pp. 868 – 873, 2022.
- [3] M. Carbonieri, D. B. Pinhal, J. Godbehere, and M. Popescu, "FEA augmented equivalent circuit for accurate performance prediction of induction machines," *International Conference on Electrical Machines* (ICEM), pp. 1 7, 2024.
- [4] O. A. Badewa, M. D. Silva, R. A. Alden, P. Asef, and D. M. Ionel, "Hybrid FEA and meta-modeling for de optimization of a highly saturated spoke IPM," *IEEE International Electric Machines Drives* Conference (IEMDC), pp. 1 – 6, 2025.
- [5] J. Rossmann, M. J. Kamper, and C. M. Hackl, "A global multi-objective bayesian optimization framework for generic machine design using gaussian process regression," *IEEE Transactions on Energy Conversion*, pp. 1 – 14, 2025.
- [6] P. Asef and C. Vagg, "A physics-informed bayesian optimization method for rapid development of electrical machines," *Scientific Reports*, vol. 4526, no. 14, 2024.
- [7] C. E. Rasmussen and C. K. I. Williams, "Gaussian processes for machine learning," vol. 18, no. 8, pp. 912 – 923, 2006.
- [8] S. Lim, Sensorless-FOC With Flux-Weakening and MTPA for IPMSM Motor Drives, TI Application Note, 2018.
- [9] S. Morimoto, M. Sanada, and Y. Takeda, "Wide-speed operation of interior permanent magnet synchronous motors with high-performance current regulator," *IEEE Transactions on Industry Applications*, vol. 30, no. 4, pp. 920 – 926, 1994.
- [10] A. Fatemi, D. M. Ionel, M. Popescu, and N. A. O. Demerdash, "Design optimization of a high torque density spoke-type PM motor for a formula E race drive cycle," *IEEE Transactions on Industry Applications*, vol. 54, no. 5, pp. 4343–4354, 2018.
- [11] A. Fatemi, Design Optimization of Permanent Magnet Machines Over a Target Operating Cycle Using Computationally Efficient Techniques. (2016). Dissertations (1934-). 662.
- [12] S. Dai, J. Song, and Y. Yue, "Multi-task bayesian optimization via gaussian process upper confidence bound," ICML 2020 Workshop on Real World Experiment Design and Active Learning, pp. 1 – 12, 2020.
- [13] Ansys® Electronics, version 25.1, 2025, ANSYS Inc.
- [14] E. V. Bonilla, K. M. A. Chai, and C. K. I. Williams, "Multi-task gaussian process prediction," *Proceedings of the 20th International Conference* on Neural Information Processing Systems, pp. 153 – 160, 2007.